# An Ultra-long Life, High-performance, Flexible Li-$CO_2$ Battery Based on Multifunctional Carbon Electrocatalysts

Li Song,[1,2,†] Chuangang Hu,[2,6,†] Ying Xiao,[3] Jianping He,[1,*] Yi Lin,[4,*] John W. Connell,[5,*] and Liming Dai[2,6*]

[1]College of Materials Science and Technology, Jiangsu Key Laboratory of Materials and Technology for Energy Conversion, Nanjing University of Aeronautics and Astronautics, 210016 Nanjing, China

[2]Center of Advanced Science and Engineering for Carbon (Case 4carbon), Department of Macromolecular Science and Engineering, Case Western Reserve University, Cleveland, OH 44106, USA

[3]BUCT-CWRU International Joint Laboratory, State Key Laboratory of Organic−Inorganic Composites, College of Energy, Beijing University of Chemical Technology, Beijing, China

[4]National Institute of Aerospace, 100 Exploration Way, Hampton, VA 23666, USA

[5]Advanced Materials and Processing Branch, NASA Langley Research Center, Hampton, VA, 23681, USA

[6]The UNSW-CWRU International Joint Laboratory, School of Chemical Engineering, University of New South Wales, Sydney, Australia

*Corresponding authors' emails: jianph@nuaa.edu.cn, yi.lin-1@nasa.gov, john.w.connell@nasa.gov, liming.dai@case.edu

[†]Authors contribute equally

**Abstract:** Integrating $CO_2$ utilization and renewable energy delivery/storage, the rechargeable Li-$CO_2$ battery has been considered as a promising candidate for next-generation secondary batteries. However, high-performance catalyst(s) for efficient formation and decomposition of the discharge product, $Li_2CO_3$, are an imperative part of a Li-$CO_2$ battery. The development of flexible Li-$CO_2$ batteries extends their applications into compliant and wearable devices/systems, but at the same time imposes a big challenge for battery fabrication and lifetime enhancement. In this study, a

rechargeable quasi-solidus flexible Li-$CO_2$ battery was designed and fabricated using highly active N,S-doped carbon nanotubes (N,S-doped CNTs) as the cathode catalyst, and a smart polymer gel as the flexible electrolyte. This newly-developed flexible Li-$CO_2$ battery exhibited a capacity as high as 23560 mAh $g^{-1}$ based on the catalyst mass and an ultra-long lifetime of up to 538 cycles with excellent mechanical flexibility. This work provides a platform for the design and development of high-performance flexible Li-$CO_2$ batteries from low-cost, earth-abundant, carbon-based multifunctional cathode catalysts.

**Keywords:** Li-$CO_2$ battery, N,S-doped carbon nanotubes, Wearable electronics, Quasi-solidus battery, Superior stability

## 1. Introduction

A Li-$CO_2$ battery provides an attractive option to capture $CO_2$ from fossil fuel combustion while it is also promising power source for space exploration on Mars with an atmosphere of ca. 96% $CO_2$ [1]. A rechargeable Li-$CO_2$ battery involves a reversible redox reaction: $4Li^+ + 3CO_2 + 4e^- \leftrightarrow C + 2Li_2CO_3$ ($E_o$ = 2.8 V vs. $Li/Li^+$) [2-4]. However, a high over-potential for reduction of $CO_2$ is often observed for the discharging process of a Li-$CO_2$ battery. For the charging process, the decomposition of insulating $Li_2CO_3$ normally leads to sluggish kinetics of the $CO_2$ evolution reaction, resulting in also a large polarization [5]. The high over-potential often causes electrolyte decomposition and consequently short cycling life for a Li-$CO_2$ battery [6]. Thus, high-

performance multifunctional catalysts for the formation and decomposition of $C/Li_2CO_3$ are required to maintain the reversible discharging/charging processes and to overcome the inherently slow reaction kinetics. Recently, Ru and Ir based catalysts have been reported to exhibit a relatively low over-potential and high cycling stability [6,7]. However, their high-cost has hindered the widespread use of these precious metal catalysts. Consequently, non-precious metals/carbon composites, such as Ni/N-doped graphene, NiO-CNT, Cu/N-doped graphene and $Mo_2C$/CNT, were also investigated [8-11], though with an unsatisfactory cycling performance of less than 150 cycles due to the unstable heterogeneous structure between the active metal sites and the carbon support. In comparison with the metal/carbon composite catalysts, the carbon-based metal-free catalysts (C-MFCs) are ideal catalysts with improved activity and durability for a Li-$CO_2$ battery. In our previous work, modified holey graphene was employed as the cathode catalyst for Li-$CO_2$ batteries, demonstrating a relatively good long-term stability of ca. 200 cycles [1,12]. In this work, with some modifications to our previous methods for synthesizing doped carbon materials [13], we utilized a simple and scalable way for the synthesis of N,S-doped CNTs as highly active, multifunctional, metal-free electrocatalysts for efficient formation and decomposition of $Li_2CO_3$.

On the other hand, all-solid-state/quasi-solid-state batteries based on ceramic/polymer electrolytes have attracted intense attention due to their multiple safety advantages, including non-flammability, non-leakage, and suppressed lithium dendrites [14]. Compared with the rigid ceramic electrolyte, the gel polymer electrolyte

is more applicable for assembling a flexible and wearable battery. Besides, the gel polymer electrolyte exhibits a high ionic conductivity comparable to that of a liquid electrolyte, which should reduce the interface impedance [15]. However, less attention has been given to flexible Li-$CO_2$ batteries with respect to their Li-ion, zinc-air and Li-$O_2$ counterparts. Recently, a flexible Li-$CO_2$ battery was developed by using wood-derived cathode coated with a Ru-loaded CNT network as the catalyst and a liquid ether (tetraglyme) electrolyte, which functioned for over 200 cycles [16]. Using non-precious metal based catalysts, Li et al. constructed quasi-solid-state flexible fiber-shaped Li-$CO_2$ batteries, which only ran for less than 50 cycles [17a], and further demonstrated it integration with dye-sensitized solar cells [17b]. Hu et al. reported a flexible Li-$CO_2$ battery involving a poly(methacrylate)/poly(ethylene glycol) based liquid-free composite polymer electrolyte [18], which showed good performance only at a relatively high temperature of 55 $^{o}$C (100 cycles). Thus, it has proven difficult to simultaneously obtain flexibility and stability for a Li-$CO_2$ battery, presumably due to the lack of an efficient catalyst and effective design of a mechanically flexible electrolyte or electrode. Using N,S-doped CNTs as the cathode catalysts and a flexible gel electrolyte as the protective coating for Li anode with no battery separator, we developed and fabricated a novel quasi-solidus, flexible, planar Li-$CO_2$ battery in this study. It was demonstrated that the multifunctional N,S-doped CNTs catalyst was highly effective in facilitating the reversible formation and decomposition of $Li_2CO_3$ in the battery. The flexible gel electrolyte not only acted as a protective coating to alleviate the detrimental chemical reactions between the Li anode and $CO_2$ from cathode but also

regulated the ion transportation through its microchannels. This design strategy led to the formation of mutually-separated particulate discharge products with a poor crystallinity, which could be readily formed and decomposed reversibly. The resultant battery exhibited a capacity as high as 23560 mAh $g^{-1}$ based on the catalyst mass at a current density of 200 mA $g^{-1}$ with an unusually good stability up to 538 cycles - outperformed all the Li-$CO_2$ batteries reported previously (Table S1). In addition, the battery could run normally and stably under various bending and folding deformation conditions, indicating outstanding flexibility/wearability.

## 2. Results and Discussion

The design of the quasi-solidus flexible planar Li-$CO_2$ battery is represented in Scheme 1. As can be seen, the flexible anode was prepared by pressing a thin lithium foil onto a stainless steel mesh to enhance the mechanical strength of the lithium foil. Thereafter, a poly(vinylidene fluoride-co-hexafluoropropylene) based gel polymer electrolyte was coated onto the lithium foil to stabilize the lithium metal and to separate the anode from cathode. The N,S-doped CNTs used as the cathode catalyst were supported on a flexible carbon cloth. Then, the pre-formed anode and cathode electrodes were heat-packed in punched aluminum-plastic films to ensure a compact contact for all the components. Fig. S1 shows typical digital photos of the quasi-solidus flexible Li-$CO_2$ batteries while the detailed procedures for the catalyst synthesis and battery assembly are provided in the Experimental Section.

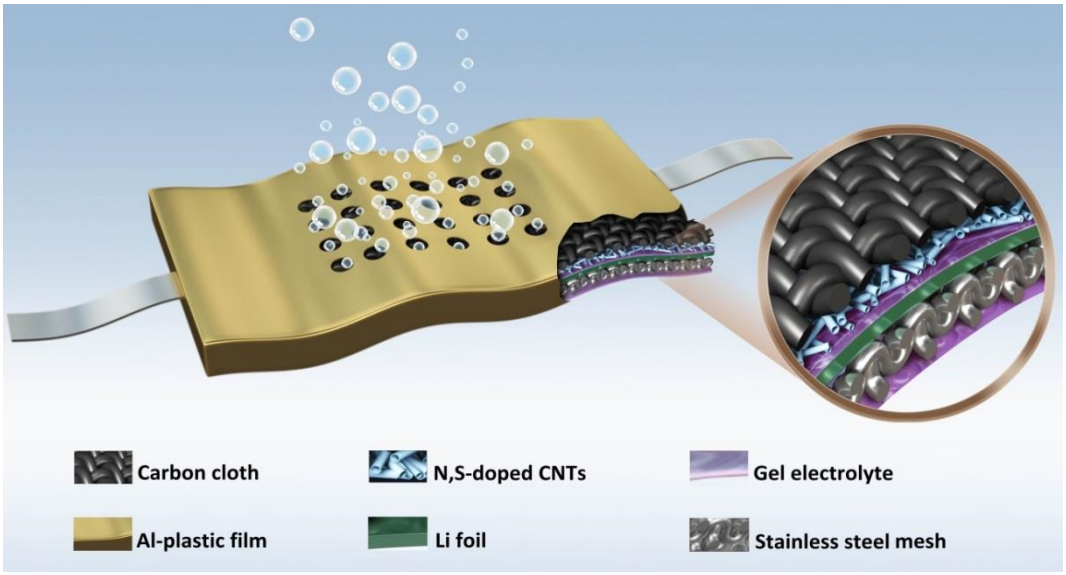


**Scheme 1.** Schematic illustration of the quasi-solidus flexible Li-$CO_2$ battery.

Fig. 1a reproduces the SEM image of the N,S-doped CNTs, which shows a 3D reticular morphology. Fig. 1b and S2 reveal a bamboo-like nanotube structure for individual CNT while Fig. 1c displays various wrinkles on the CNT walls, which could enhance the available electrochemical active surface area and the defect-induced electrocatalytic activities. As shown in Fig. 1d-g, both nitrogen and sulfur are uniformly doped over the entire CNT framework. Fig. S3 shows that the N,S-doped CNTs, when coated on the carbon cloth, stacked and cross-linked together to provide sufficient space for facilitating $CO_2$ diffusion and discharge product storage. The X-ray photoelectron spectroscopic (XPS) survey spectrum and high-resolution XPS C1s spectrum in Fig. S4a and S4b further demonstrate the successful doping of N and S into the CNTs with a doping content of 4.1 at% and 0.73 at% for N and S, respectively. The corresponding high-resolution N1s spectrum given in Fig. 1h shows mainly the pyridine and graphitic

nitrogen [19]. The high-resolution XPS S 2p spectrum in Fig. 1i can be deconvoluted into three characteristic peaks of -C-S-C-, -C=S- and -$SO_n$-, respectively [20]. The high-resolution XPS O 1s (7.7 at%) spectrum shown in Fig. S4c is deconvoluted into O=C, O–C, and O–N, respectively [21]. We have also performed Brunauer-Emmett-Teller (BET) surface area measurement on the N,S-doped CNTs to characterize their porosity. Fig. 1j shows the typical type-IV hysteresis loop for a mesoporous structure with mainly ~5-nm pores favorable for $CO_2$ adsorption and ion infiltration. Also, carbon nanotube characteristics can be seen from the corresponding XRD pattern and Raman spectrum in Fig. S5a and S5b, respectively [22].

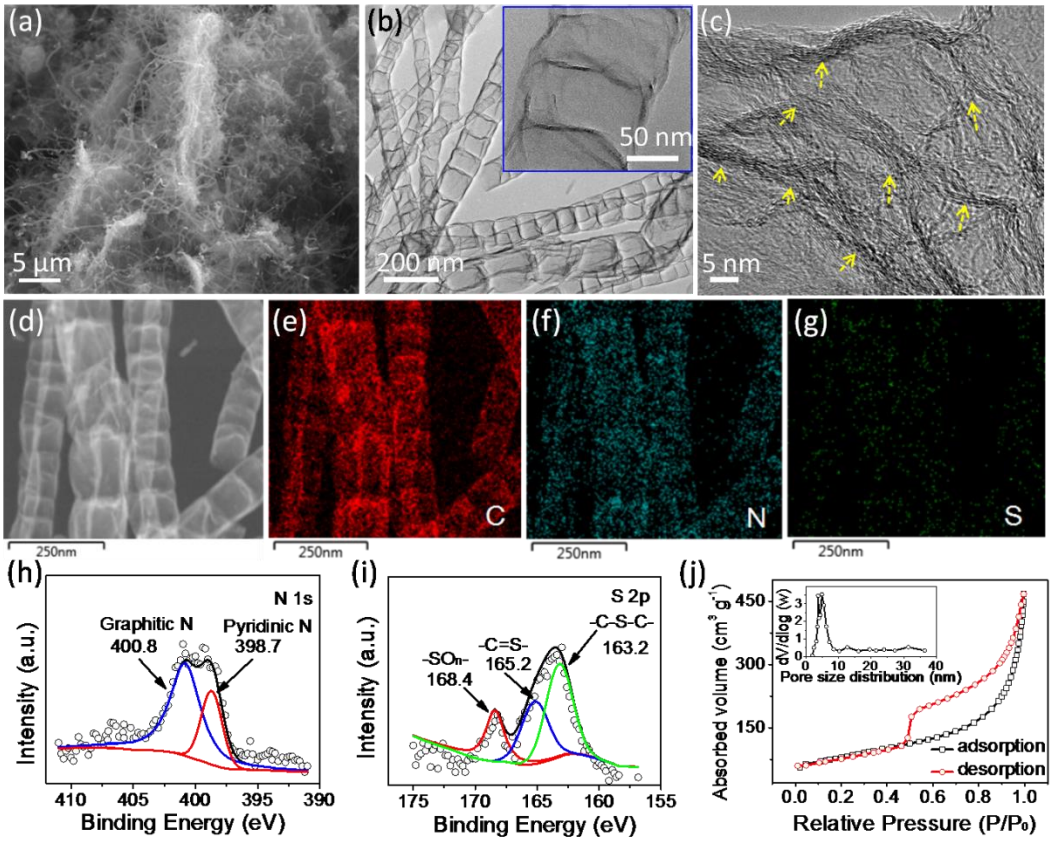


**Fig. 1.** (a) SEM image, (b, c) TEM images, (d) high-angle annular dark-field scanning transmission electron microscope HAADF-STEM image and (e-g) element mapping images of the N,S-doped

CNTs. High-resolution XPS spectra of (h) N 1s and (i) S 2p for the N,S-doped CNTs. (j) Nitrogen adsorption-desorption curves and the corresponding pore size distribution (inset) of the N,S-doped CNTs.

To investigate electrocatalytic performance of N,S-doped CNTs and other kinds of CNTs, we first assembled them into a rechargeable Li-$CO_2$ coin cell with a liquid electrolyte (*i.e.*, 1 M LiTFSI in dimethyl sulfoxide). N-doping of graphitic carbon has been widely demonstrated to induce elctrocatalytic activities through charge transfer from the adjacent conjugated carbon atoms to facilitate reduction reactions [17a, 23], specifically $CO_2$ reduction for the $Li_2CO_3$ deposition during discharging in this particular case. Furthermore, co-doping with S atoms of a different spin density from that of carbon atoms could induce active sites for $CO_2$ evolution [24], leading to the formation of N,S-doped bifunctional carbon electrocatalysts for reversible Li-$CO_2$ batteries developed in this study. As displayed in Fig. S6a, the battery with an N,S-doped CNT cathode delivered a high capacity of 6682 mAh $g^{-1}$ at a current density of 200 mA $g^{-1}$, superior to the commercial, undoped CNT and N-doped CNT counterparts. The corresponding battery under an Ar atmosphere exhibited a negligible capacity during discharge (Fig. S6b), indicating that the observed high capacity for the N,S-doped CNT Li-$CO_2$ battery came from the reduction of $CO_2$ catalyzed by the N,S-doped CNTs. The N,S-doped CNT battery could be reversibly discharged and charged up to 103 cycles whereas only 51 stable cycles were achieved for the N-doped CNT battery (Fig. S7). In order to gain a deep understanding of the reversibility of the N,S-doped

CNT Li-$CO_2$ battery, we further carried out XRD and Raman measurements on the cathodes after charge and discharge, respectively. The XRD patterns (Fig. S8) and Raman spectra (Fig. S9) reveal the reversible formation and decomposition of $Li_2CO_3$ (characteristic XRD peaks, PDF-22-1141) on the N,S-doped CNT cathode. Fig. S10b and S11b show the deposition of $Li_2CO_3$ products over the N,S-doped CNTs network after discharge. Upon recharge, the $Li_2CO_3$ products largely vanished, leaving only a few $Li_2CO_3$ nanoparticles on the CNT cathode (Fig. S10c and S11c). These results clearly indicate excellent multifunctional catalytic activities of the N,S-doped CNTs to catalyze the reversible formation and decomposition of $Li_2CO_3$.

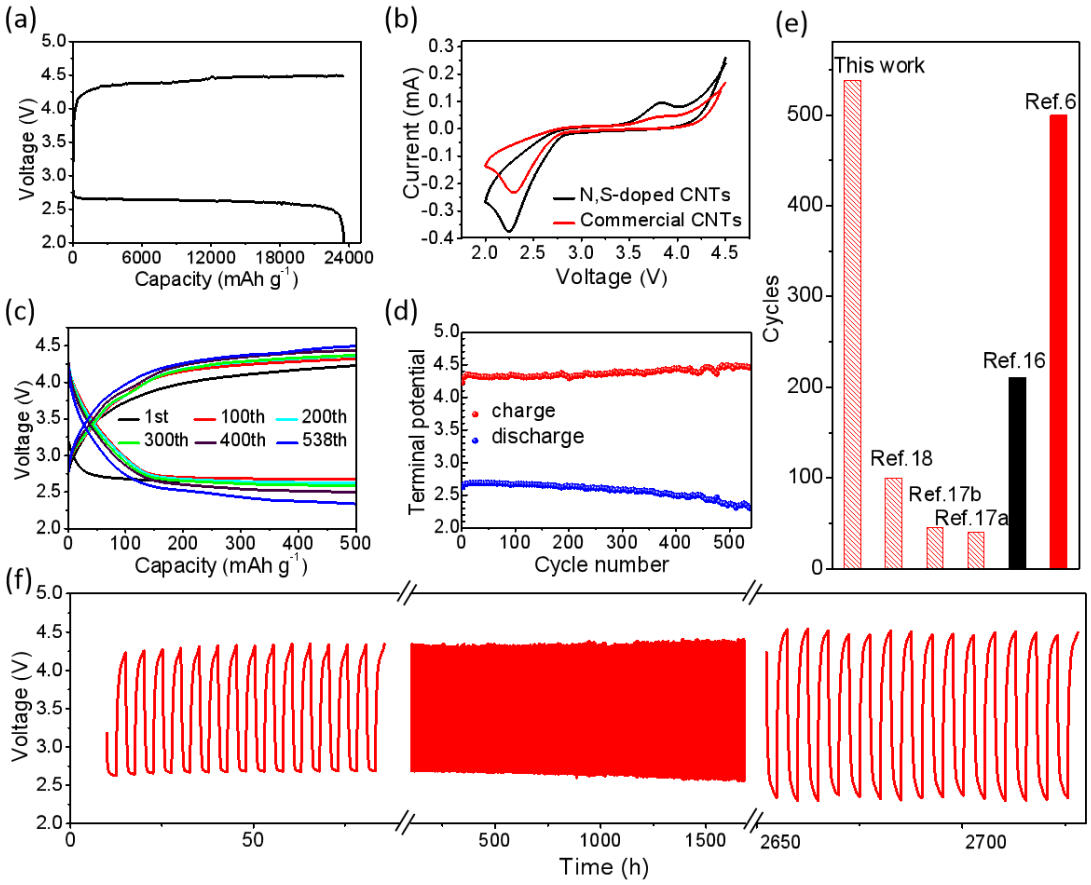


**Fig. 2.** (a) Full discharge and charge curves. (b) CV curves of the quasi-solidus flexible Li-$CO_2$ batteries using the N,S-doped CNTs and commercial CNTs as catalysts at a scanning rate of 0.1 mV

$s^{-1}$. (c) Discharge-charge profiles at different cycles of the N,S-doped CNT quasi-solidus Li-$CO_2$ battery with the 500 mAh $g^{-1}$ capacity limitation at a current density of 200 mA $g^{-1}$ with the terminal discharge/charge potentials of 2.3 and 4.5 V. (d) Terminal discharge/charge potentials over 538 cycles. (e) The cycling life of the quasi-solidus flexible Li-$CO_2$ battery in this work in comparison with the corresponding results in the recent literature. ▧ Quasi-solidus flexible battery, ■ Liquid flexible battery, ■ The currently reported liquid battery with the best cyclic stability in the literature. (f) Time-voltage curves during the whole discharge/charge cycling process.

The aforementioned results from the liquid battery prompted us to design and construct quasi-solidus flexible batteries using the gel polymer electrolyte (see, Experimental Section). As shown in Fig. 2a, the quasi-solidus flexible Li-$CO_2$ battery exhibited a specific capacity of 23560 mAh $g^{-1}$ with a long discharge and charge plateau at around 2.63 and 4.3 V, respectively – superior to its counterparts based on the CNT (Fig. S12) and the N,S-doped CNT liquid battery (Fig. S6a). Fig. 2b shows a couple of remarkable redox peaks, corresponding to the reduction of $CO_2$ and decomposition of $Li_2CO_3$, for the flexible Li-$CO_2$ battery based on the N,S-doped CNTs. Compared with the CNTs, the N,S-doped CNTs also show improved onset potentials and peak currents. Furthermore, Fig. 2c shows stable charge/discharge reversibility up to 538 cycles, indicating a much better long-term cycling stability than that of the liquid battery (*cf.* Fig. S7). The corresponding terminal discharge and charge potentials derived from Fig. 2c are displayed in Fig. 2d, exhibiting a very slow polarization enlargement over the entire 538 cycles. As shown in Fig. 2e and Table S1, our flexible Li-$CO_2$ battery based on the N,S-doped CNTs exhibited much better stability than all other reported Li-$CO_2$

batteries [6,16-18]. The voltage-time response for the whole 538 cycles is given in Fig. 2f, which shows that our flexible battery could stably work for over 110 days, presumably because the gel electrolyte can provide better protection than the liquid electrolyte to retard the $CO_2$ penetration, and hence no Li anode corrosion or undesired side reactions [25].

To evaluate the rate capability, we first ran the N,S-doped CNT flexible Li-$CO_2$ battery at progressively enlarged current densities, ranging from 200 to 2000 mA $g^{-1}$ (Fig. 3a). Thereafter, the current density was decreased to 50 mA $g^{-1}$ and then increased to 200 mA $g^{-1}$. It is found in Fig. 3b that the over-potential increased slowly with the increasing current, and retained the original values when the current was reduced to 200 mA $g^{-1}$, indicating an excellent rate capability. To investigate possible changes of the cathode, we recorded XRD patterns and Raman spectra at different stages of the discharging-charging processes. Similar to the liquid battery (cf. Fig. S8 and S9), Fig. 3c and 3d for the flexible Li-$CO_2$ battery also show reversible appearance and disappearance of $Li_2CO_3$, albeit somewhat less obvious. It is worthwhile to note that the XRD peak intensity of the $Li_2CO_3$ in this quasi-solidus battery is much weaker than that of the liquid battery, though the same catalyst loading was used in both cases.

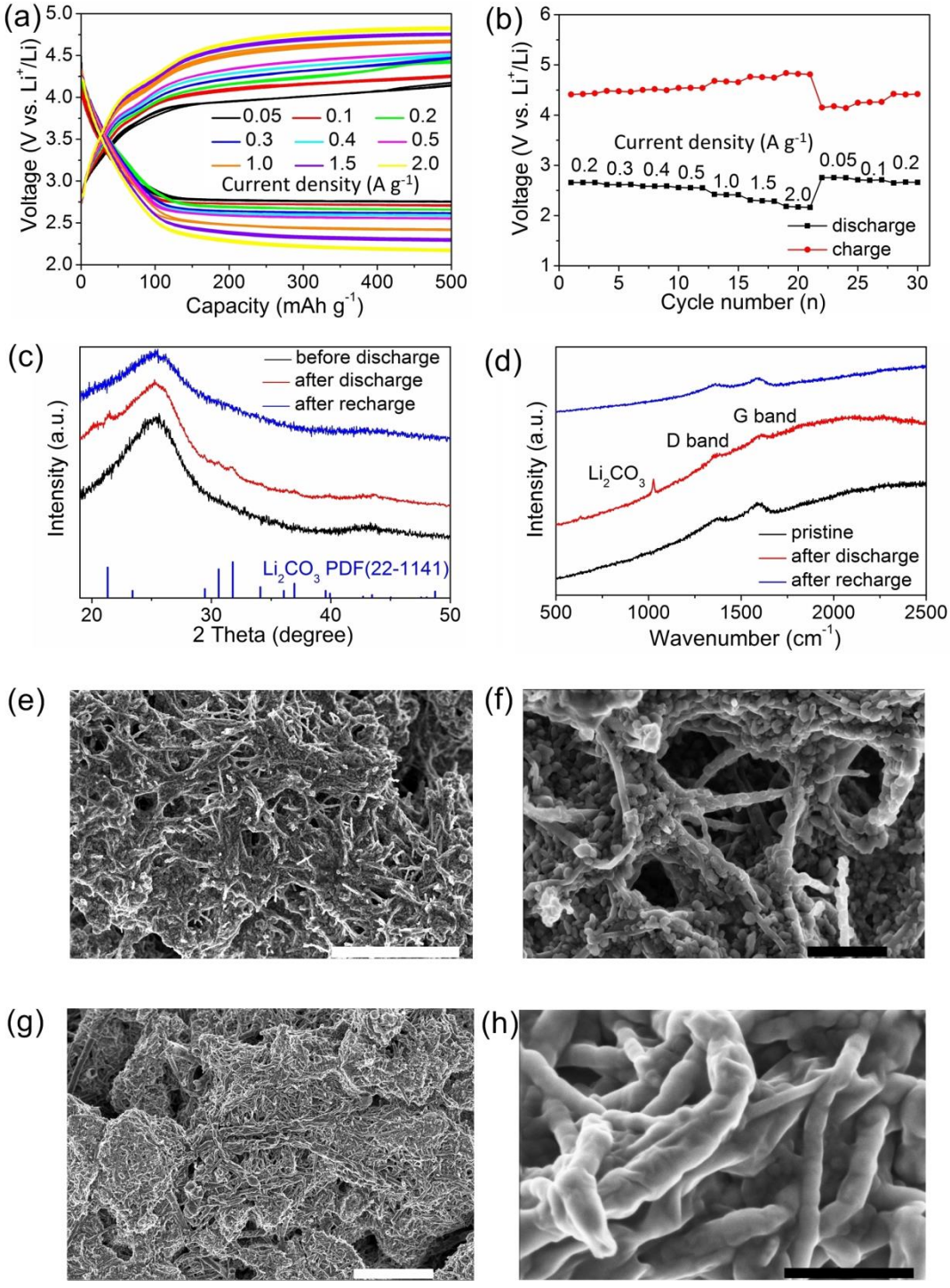


**Fig. 3.** Performance of the quasi-solidus flexible Li-$CO_2$ battery using N,S-doped CNTs. (a) Discharge-charge curves and (b) the discharge/charge terminal voltages derived from (a) at different current densities (A $g^{-1}$). (c) XRD patterns and (d) Raman spectra at different states. SEM images of the N,S-doped CNT electrode after (e, f) discharging and (g, h) recharging process, respectively. Scale bars: (e) 4 μm, (f) 500 nm, (g) 5 μm and (h) 400 nm.

As can be seen in Fig. 3f, there are many small $Li_2CO_3$ particles uniformly distributed on the outer walls of the N,S-doped CNTs after discharge, and all the discharge products are removed by recharging (Fig. 3g-h) the flexible Li-$CO_2$ battery. The discharge particles with a relatively poor crystallinity and small size in the flexible Li-$CO_2$ were readily decomposed during the charging process, leading to a decreased polarization (Fig. S13) and increased stability during the charge/discharge cycles. A simple comparison of the EIS spectra in Fig. S14 with those in Fig. S15 shows that the liquid Li-$CO_2$ battery exhibited a much larger resistance increase after discharging process than that of the quasi-solidus flexible Li-$CO_2$ battery due to the accumulation of the continuous polymer-like insulating $Li_2CO_3$ products on the entire cathode electrode in the former. As a result, the liquid ether electrolyte-based battery could run for only 126 cycles even at a relatively larger cut-off voltage range (Fig. S16). Clearly, therefore, the quasi-solidus flexible Li-$CO_2$ battery has a better cyclability than that of the liquid battery.

Employed as a flexible device, our quasi-solidus battery can stably operate at various deformation conditions. Fig. 4a shows an open potential of 3.13 V for the quasi-solidus flexible Li-$CO_2$ battery, which is close to the typical potential of a Li/C full cell.[19] Fig. 4b and Fig. S17 show that an LED cinema lightbox with a nominal voltage of 6 V could be powered by two such batteries in series. The quasi-solidus flexible battery could continue to normally function even when bent and flexed, including tortuous conditions (Fig. 4c) and folding deformations (Fig. 4d), demonstrating the robustness and

flexibility of both the electrodes and gel electrolyte.

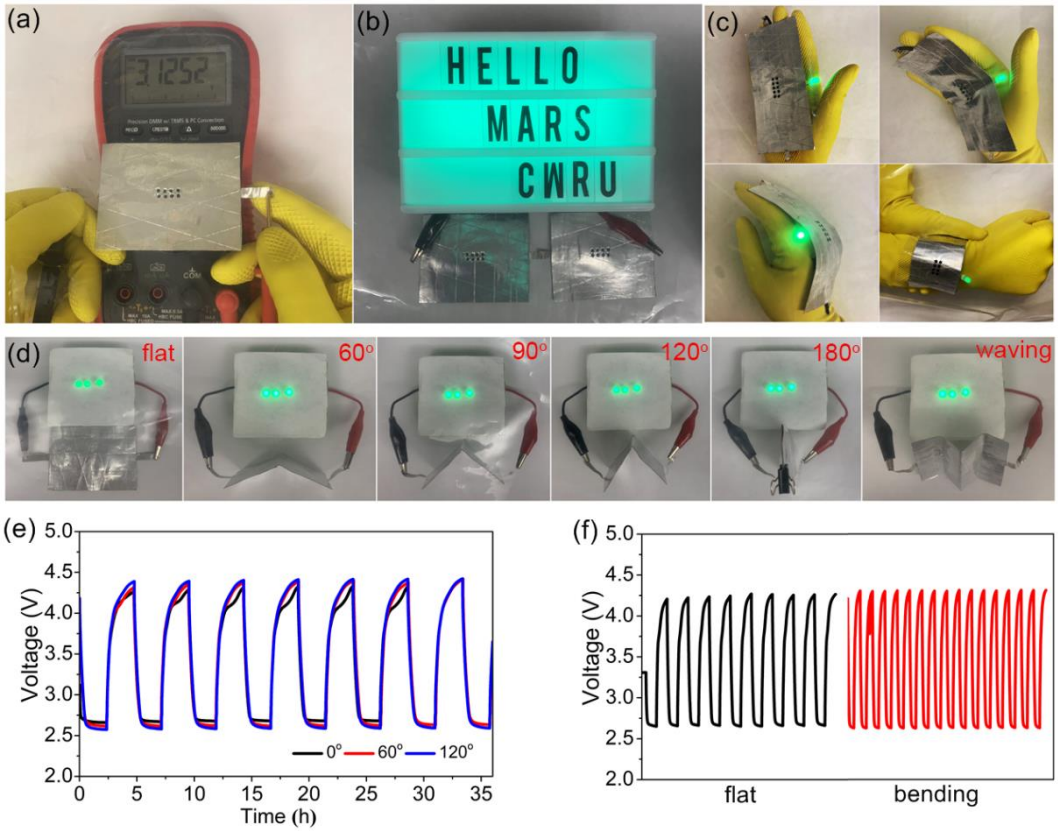


**Fig. 4.** (a) Open potential of a quasi-solidus flexible Li-$CO_2$ battery based on the N,S-doped CNT cathode. (b) An LED cinema lightbox powered by two such batteries in series. Photos of the flexible Li-$CO_2$ battery lighting up the LED bulb (c) under wearable conditions and (d) under various folding deformations. Discharge-charge profiles of the flexible Li-$CO_2$ battery (e) at various folding angles, and (f) under flat/bending conditions. All the photos were obtained in a glove-bag filled with $CO_2$ and the electrochemical measurements were tested in a sealed bottle filled with $CO_2$.

We further tested the cycling stability under different deformation states. As can be seen in Fig. 4e, the folded batteries displayed a slightly higher polarization compared with the flat battery. Fig. 4f shows that the quasi-solidus flexible Li-$CO_2$ battery under a bending state still displayed very stable voltage-time profiles. We tested the EIS spectra of this flexible battery under different deformations to find out if it would cause any difference in the charge transport capability. As shown in Fig. S18, the 60$^o$ and

120$^{o}$ folded batteries exhibited a bit larger resistance than that of the flat one. However, the resistance decreased to the original value when the battery was returned to the flat state. The observed high mechanical flexibility of this quasi-solidus battery is attributable to the delicate design of the flexible electrode structure and the utilization of the gel electrolyte, thus helping to keep both intimate contact and stable structure of the battery assembly under various deformation states.

In summary, a quasi-solidus flexible Li-$CO_2$ battery was developed and systematically studied. Due to the efficient multifunctional activity of the N,S-doped carbon-nanotubes, the regulated Li ion transportation method and ability to prevent anode fouling provided by the smart gel electrolyte, combined with delicate design of the battery configuration, the resulting quasi-solidus flexible Li-$CO_2$ battery delivered an extremely high capacity of 23560 mAh $g^{-1}$, and could work with an ultra-long life-time for more than 110 days. Furthermore, the battery can be run under different deformations without performance decay. This work provides an innovative strategy to design a promising quasi-solidus flexible metal-air battery and to develop highly active and low-cost catalysts for Li-$CO_2$ batteries.

## Appendix A: Supplementary material

Further experimental details and illustration of relaxed structures, are provided in the Supporting Information online.

**Acknowledgements**

This work was financially supported by NASA (NNX16AD48A and NNC16CA42C). Li Song was supported by the National Natural Science Foundation of China (11575084 and 51602153), Funding of Jiangsu Innovation Program for Graduate Education (KYCX17_0250), Funding for Outstanding Doctoral Dissertation in NUAA (BCXJ17-09) and A Project Funded by the Priority Academic Program Development of Jiangsu Higher Education Institutions (PAPD). Partial funding from ARC (DP 190103881 and FL 190100126) is also acknowledged.

**Competing financial interests:**

The authors declare no competing financial interests.

**References**

[1] L. Qie, Y. Lin, J. W. Connell, J. Xu, L. Dai, Highly rechargeable lithium-$CO_2$ batteries with a boron-and nitrogen-codoped holey-graphene cathode, *Angew. Chem. Int. Ed.* **56** (2017), 6970-6974.

[2] Z. Zhang, Q. Zhang, Y. Chen, J. Bao, X. Zhou, Z. Xie, J. Wei, Z. Zhou, The first introduction of graphene to rechargeable Li-$CO_2$ batteries, *Angew. Chem. Int. Ed.* **54** (2015), 6550-6553.

[3] J. Chen, K. Zou, P. Ding, J. Deng, C. Zha, Y. Hu, X. Zhao, Conjugated cobalt polyphthalocyanine as the elastic and reprocessable catalyst for flexible Li-$CO_2$ batteries, *Adv. Mater.* **31** (2019), 1805484.

[4] Y. Qiao, J. Yi, S. Wu, Y. Liu, S. Yang, P. He, H. Zhou, Li-$CO_2$ electrochemistry: a new strategy for $CO_2$ fixation and energy storage, *Joule* **1** (2017), 359-370.

[5] C. Ling, R. Zhang, K. Takechi, F. Mizuno, Intrinsic barrier to electrochemically decompose $Li_2CO_3$ and LiOH, *J. Phys. Chem. C* **118** (2014), 26591-26598.

[6] Y. Xing, Y. Yang, D. Li, M. Luo, N. Chen, Y. Ye, J. Qian, L. Li, D. Yang, F. Wu, Crumpled Ir nanosheets fully covered on porous carbon nanofibers for long-life rechargeable lithium-$CO_2$ batteries, *Adv. Mater.* **30** (2018), 1803124.

[7] S. Yang, Y. Qiao, P. He, Y. Liu, Z. Cheng, J.-j. Zhu, H. Zhou, A reversible lithium-$CO_2$ battery with Ru nanoparticles as a cathode catalyst, *Energy Environ. Sci.* **10** (2017), 972-978.

[8] Z. Zhang, X. G. Wang, X. Zhang, Z. Xie, Y. N. Chen, L. Ma, Z. Peng, Z. Zhou, Verifying the rechargeability of Li-$CO_2$ batteries on working cathodes of Ni nanoparticles highly dispersed on N-doped graphene, *Adv. Sci.* **5** (2018), 1700567.

[9] X. Zhang, C. Wang, H. Li, X.-G. Wang, Y.-N. Chen, Z. Xie, Z. Zhou, High performance Li-$CO_2$ batteries with NiO-CNT cathodes, *J. Mater. Chem. A* **6** (2018), 2792-2796.

[10] Z. Zhang, Z. Zhang, P. Liu, Y. Xie, K. Cao, Z. Zhou, Identification of cathode stability in Li-$CO_2$ batteries with Cu nanoparticles highly dispersed on N-doped graphene, *J. Mater. Chem. A* **6** (2018), 3218-3223.

[11] Y. Hou, J. Wang, L. Liu, Y. Liu, S. Chou, D. Shi, H. Liu, Y. Wu, W. Zhang, J. Chen,

$Mo_2C$/CNT: an efficient catalyst for rechargeable Li–$CO_2$ batteries, *Adv. Funct. Mater.* **27** (2017), 1700564.

[12] Y. Jin, C. Hu, Q. Dai, Y. Xiao, Y. Lin, J. W. Connell, F. Chen, L. Dai, High-performance Li-$CO_2$ batteries based on metal-free carbon quantum dot/holey graphene composite catalysts, *Adv. Funct. Mater.* **28** (2018), 1804630.

[13] (a) C. Hu, L. Dai, Multifunctional carbon-based metal-free electrocatalysts for simultaneous oxygen reduction, oxygen evolution, and hydrogen evolution, *Adv. Mater.* **29** (2017), 1604942; (b) C. Hu, X. Chen, Q. Dai, M. Wang, L. Qu, L, Earth-abundant carbon catalysts for renewable generation of clean energy from sunlight and water, *Nano Energy* **41** (2017), 367-376; (c) C. Hu, L. Wang, Y. Zhao, M. Ye, Q. Chen, Z. Feng, L. Qu, Designing nitrogen-enriched echinus-like carbon capsules for highly efficient oxygen reduction reaction and lithium ion storage, *Nanoscale* **6** (2014), 8002-8009.

[14] W. Zhou, S. Wang, Y. Li, S. Xin, A. Manthiram, J. B. Goodenough, Plating a dendrite-free lithium anode with a polymer/ceramic/polymer sandwich electrolyte, *J. Am. Chem. Soc.* **138** (2016), 9385-9388.

[15] (a) Y. Zhang, L. Wang, Z. Guo, Y. Xu, Y. Wang, H. Peng, High-performance lithium-air battery with a coaxial-fiber architecture, *Angew. Chem. Int. Ed.* **55** (2016), 4487-4491; (b) Y. Jin, X. Liu, S. Guo, K. Zhu, H. Xue, H. Zhou, Novel stable gel polymer electrolyte: toward a high safety and long life Li-air battery, *Appl. Mater. Interfaces* **7** (2015), 23798-23804.

[16] S. Xu, C. Chen, Y. Kuang, J. Song, W. Gan, B. Liu, E. M. Hitz, J. W. Connell, Y. Lin, L. Hu, Flexible lithium-$CO_2$ battery with ultrahigh capacity and stable cycling, *Energy Environ. Sci.* **11** (2018), 3231-3237.

[17] (a) Y. Li, J. Zhou, T. Zhang, T. Wang, X. Li, Y. Jia, J. Cheng, Q. Guan, E. Liu, H. Peng, B. Wang, Highly surface-wrinkled and N-doped CNTs anchored on metal wire: A novel fiber-shaped cathode toward high-performance flexible Li-$CO_2$ batteries, *Adv. Funct. Mater.* 29 (2019), 1808117. (b) X. Li, J. Zhou, J. Zhang, M. Li, X. Bi, T. Liu, Tao, He, J. Cheng, F. Zhang, Y. Li, X. Mu, J. Lu, B. Wang, Li–$CO_2$ Batteries: Bamboo-Like Nitrogen-Doped Carbon Nanotube Forests as Durable Metal-Free Catalysts for Self-Powered Flexible Li–$CO_2$ Batteries, *Adv. Mater.* (2019) https://doi.org/10.1002/adma.201970279.

[18] X. Hu, Z. Li, J. Chen, Flexible Li-$CO_2$ batteries with liquid-free electrolyte, *Angew. Chem. Int. Ed.* **56** (2017), 5785-5789.

[19] (a) W. Niu, L. Li, X. Liu, N. Wang, J. Liu, W. Zhou, Z. Tang, S. Chen, Mesoporous N-doped carbons prepared with thermally removable nanoparticle templates: an efficient electrocatalyst for oxygen reduction reaction, *J. Am. Chem. Soc.* **137** (2015), 5555-5562; (b) Z. Pei, H. Li, Y. Huang, Q. Xue, Y. Huang, M. Zhu, Z. Wang, C. Zhi, Texturing in situ: N, S-enriched hierarchically porous carbon as a highly active reversible oxygen electrocatalyst, *Energy Environ. Sci.* **10** (2017), 742-749.

[20] (a) J. Liang, Y. Jiao, M. Jaroniec, S. Z. Qiao, Sulfur and nitrogen dual-doped mesoporous graphene electrocatalyst for oxygen reduction with synergistically

enhanced performance, *Angew. Chem. Int. Ed.* **51** (2012), 11496-11500; (b) Y. Zhang, M. Chu, L. Yang, W. Deng, Y. Tan, M. Ma, Q. Xie, Synthesis and oxygen reduction properties of three-dimensional sulfur-doped graphene networks, *Chem. Commun.* **50** (2014), 6382-6385; (c) Y. Li, H. Zhang, Y. Wang, P. Liu, H. Yang, X. Yao, D. Wang, Z. Tang, H. Zhao, A self-sponsored doping approach for controllable synthesis of S and N co-doped trimodal-porous structured graphitic carbon electrocatalysts, *Energy Environ. Sci.* **7** (2014), 3720-3726; (d) J. Shao, X. Li, L. Zhang, Q. Qu, H. Zheng, Core-shell sulfur@polypyrrole composites as high-capacity materials for aqueous rechargeable batteries, *Nanoscale* **5** (2013), 1460-1464; (e) W. Kiciński, M. Szala, M. Bystrzejewski, Sulfur-doped porous carbons: synthesis and applications, *Carbon* **68** (2014), 1-32.

[21] (a) J. Fu, B. Zhu, C. Jiang, B. Cheng, W. You, J. Yu, Hierarchical porous O-doped g-$C_3N_4$ with enhanced photocatalytic $CO_2$ reduction activity, *Small* **13** (2017), 1603938; (b) B. Duan, X. Gao, X. Yao, Y. Fang, L. Huang, J. Zhou, L. Zhang, Unique elastic N-doped carbon nanofibrous microspheres with hierarchical porosity derived from renewable chitin for high rate supercapacitors, *Nano Energy* **27** (2016), 482-491.

[22] J. Meng, C. Niu, L. Xu, J. Li, X. Liu, X. Wang, Y. Wu, X. Xu, W. Chen, D. Zhao, L. Mai, General oriented formation of carbon nanotubes from metal-organic frameworks, *J. Am. Chem. Soc.* **139** (2017), 8212-8221.

[23] J. Zhang, Z. Xia, L. Dai, Carbon-based electrocatalysts for advanced energy

conversion and storage, *Sci. Adv.* **1** (2015), e1500564, and references cited therein.

[24] C. Hu, Y. Xiao, Y. Z, L. Dai, Carbon-based metal-free electrocatalysis for energy conversion, energy storage, and environmental protection, *Electrochemical Energy Reviews* **1** (2018), 84–112, and references cited therein.

[25] C. Li, Z. Guo, B. Yang, Y. Liu, Y. Wang, Y. Xia, A rechargeable Li-$CO_2$ battery with a gel polymer electrolyte, *Angew. Chem. Int. Ed.* **56** (2017), 9126-9130.

# Supporting Information

# An Ultra-long Life, High-performance, Flexible Li-$CO_2$ Battery Based on Multifunctional Carbon Electrocatalysts

**Experimental Methods**

**Chemicals:**

Lithium bis(trifluoromethane sulfonimide) (LiTFSI, 99.95%), tetraethylene glycol dimethyl ether (TEGDME, tetraglyme, 99.9%), poly(vinylidene fluoride-co-hexafluoropropylene) (PVDF-HFP, Mn=130,000), dimethyl sulfoxide (DMSO, anhydrous, 99.9%), trimethylolpropane ethoxylate triacrylate (TMPET), 2-hydroxy-2-methyl-1-phenyl-1-propanone (HMPP) and 1-Methyl-2-pyrrolidinone (NMP, anhydrous, 99.5%) were purchased from Sigma-Aldrich and used without any further purification.

**Materials synthesis:**

In a typical procedure, 2.0 g of $FeCl_3 \cdot 6H_2O$ powders were dissolved into 50 mL of deionized water to form a transparent solution, followed by adding 30 g of melamine. After vigorous stirring for 12 h, Fe ions adsorbed onto melamine particles by the coordination between the metal cations and abundant amino groups, and were collected by lyophilization. Subsequently, 5.0 g of trithiocyanuric acid was well mixed with above dried powder and then placed in the center of a quartz tube

furnace. The temperature was ramped at 3 $^{o}$C min$^{-1}$ up to 900 $^{o}$C with the feeding of Ar (200 s.c.c.m.) at ambient pressure (s.c.c.m., standard cubic centimeters per minute). After cooling to room temperature under Ar protection, the resulting sample was treated with hydrochloric acid solution (9 M) and nitric acid (3 M) at 60 $^{o}$C for 24 h to remove the redundant Fe nanoparticles. Finally, the sample was obtained by repeatedly washing with deionized water and lyophilization. The control sample of N doped carbon nanotubes (N-doped CNTs) was prepared with the same treatment except S precursor (trithiocyanuric acid) powders were introduced during the annealing process.

**Physical Characterization:**

Phase characterization was conducted by X-ray diffraction (XRD) with a Miniflex II diffractometer at a scan rate of 1$^{o}$ min$^{-1}$. The structures and morphologies were observed by transmission electron microscopy (TEM, ZeissLibra 200EF) and scanning electron microscopy (SEM, HitachiS-5200). X-ray photoelectron spectroscopy (XPS, PHI Versaprobe 5000) was performed to reveal the element content and oxidation states of the catalyst. Raman spectroscopy (Renishaw, 514 nm laser) was measured to characterize the structure of carbon nanotubes and lithium carbonate. The $N_2$ adsorption/desorption isotherms were collected using an AutoSorb iQ2 analyzer at 77 K. The batteries under different states were disassembled to obtain the cathodes, which were characterized by XRD, SEM and Raman spectroscopy.

**Battery Assembly and Electrochemical Measurements:**

To fabricate the quasi-solidus flexible Li-$CO_2$ battery, the gel polymer electrolyte was first prepared. The gel polymer electrolyte consisted of LiTFSI/TEGDME Li salt liquid electrolyte, polymer solution PVDF-HFP/NMP and photoinitiator HMPP/TMPET, which helps to cure the precursor solution to a

quasi-solidus gel state using UV irradiation. Typically, 1.0 g PVDF-HFP was dissolved in 4.0 g NMP to form the sol matrix. 10 ul HMPP dissolved in 3.0 g TMPET was used as the photoinitiator. 1 M LiTFSI in TEGDME was used as its liquid lithium salt electrolyte. The above three solutions were mixed together with a mass ratio of 5:3:4 to form the gel electrolyte precursor. The lithium foil was depressed on a 304 stainless steel mesh (purchased from Changzhou Leikou Metalware Co., LTD, 400 mesh, with the wire diameter, pore diameter and thickness of 30 μm, 30 μm and 60 μm, respectively) serving as the anode. Afterwards, the Li-foil contained stainless steel mesh was dipped into the gel electrolyte precursor and subsequently cured under UV irradiation with 365 nm wavelength for 15 s. This step was conducted twice to obtain a solidified and flexible Li-gel anode. The above procedures were conducted in an argon-filled glove box. The catalyst inks were prepared by dispersing 5 mg N,S-doped CNTs or other control samples in 1 mL of isopropanol containing 50 ul 5 wt.% Nafion solution. A flexible carbon cloth was employed as the gas diffusion layer and current collector, on which the catalyst ink was pipetted with a total loading of 0.2 mg. Then the air-cathode was dried under vacuum for 10 h. Finally, the anode and cathode were assembled inside the aluminum plastic films with several air holes punched on the cathode side and hot-pressed into a planar pouch-type flexible Li-$CO_2$ battery in the argon-filled glove box. The liquid battery was assembled in the form of 2032-type coin cell with a Li foil anode, an air-cathode with the catalysts supported on the carbon paper and a glass-fiber separator impregnated with 1 M LiTFSI dissolved in dimethyl sulfoxide (DMSO) unless otherwise noted. For the purposes of comparison, 1 M LiTFSI in TEGDME is also employed as another liquid electrolyte. The catalyst ink was pipetted on the carbon paper with the same loading of 0.2 mg. The battery performance measurements were performed through a multichannel battery testing system (Land). We tested

the cells in a $CO_2$-filled bottle, which was inflated with $CO_2$ to positive pressure. So we could determine whether there was air leakage during the battery test by perception of the pressure when we opened the bottle. The glove-bag was also filled with $CO_2$ and used to display the various scenes in which the flexible batteries worked. All the mentioned voltages are versus $Li^+/Li$. All the current densities as well as the specific capacities for the batteries were normalized to the mass loading of the CNTs catalysts on the gas electrode. EIS measurements for the battery were conducted on an electrochemical workstation (CHI 760E) at the open circuit potential with the frequency ranging from $10^5$ Hz to $10^{-2}$ Hz.

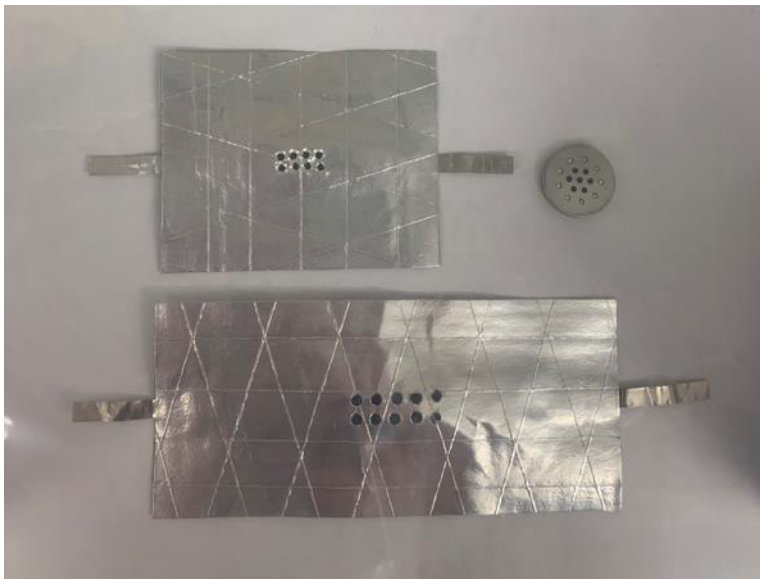

**Fig. S1.** The digital photos of the quasi-solidus planar Li-$CO_2$ battery with different sizes and a coin-cell liquid electrolyte Li-$CO_2$ battery.

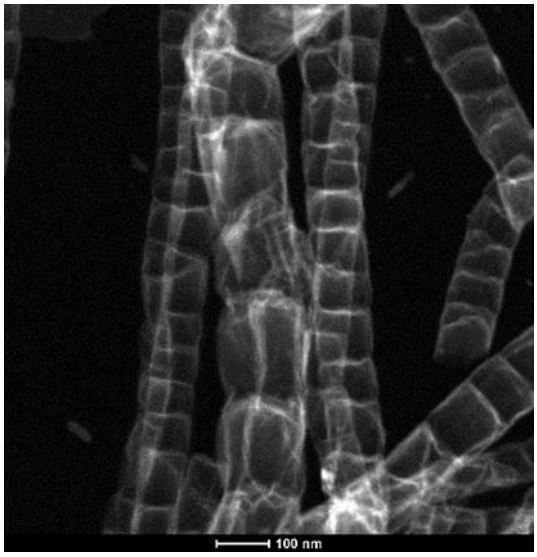


**Fig. S2.** STEM image of N,S-doped CNTs.

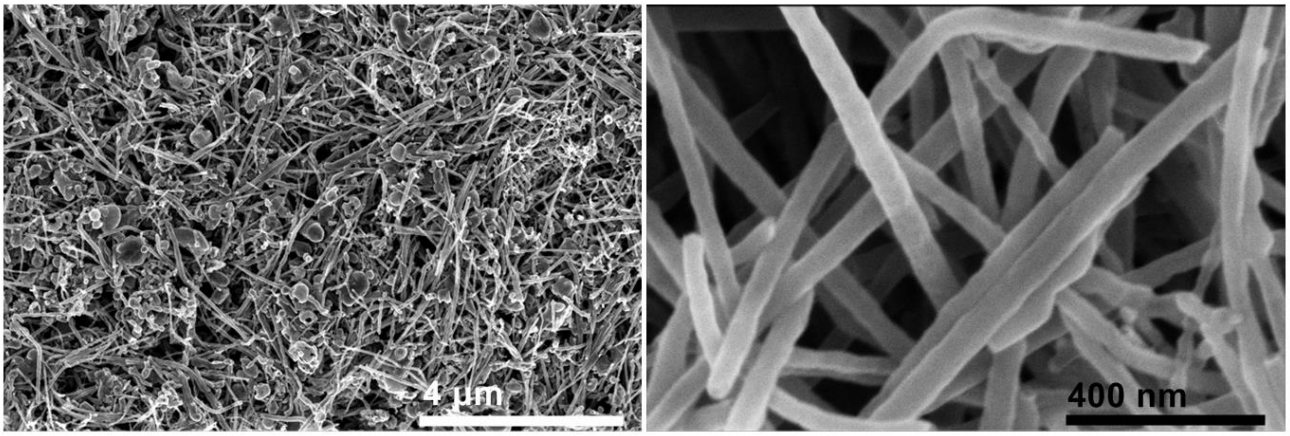


**Fig. S3.** SEM images of the N-S-doped CNTs catalysts-supported cathode on the carbon cloth.

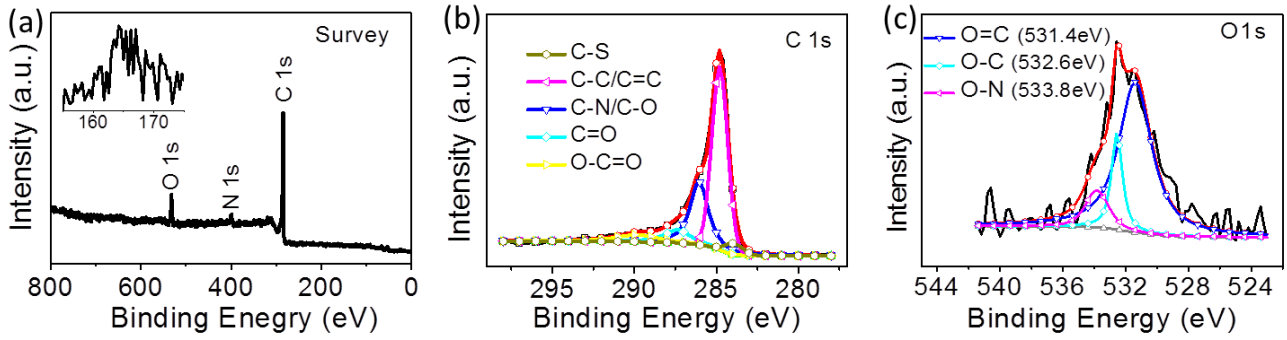


**Fig. S4.** (a) XPS survey spectrum of N,S-doped CNTs. High resolution XPS spectrum of (b) C 1s and (c) O 1s of N,S-doped CNTs.

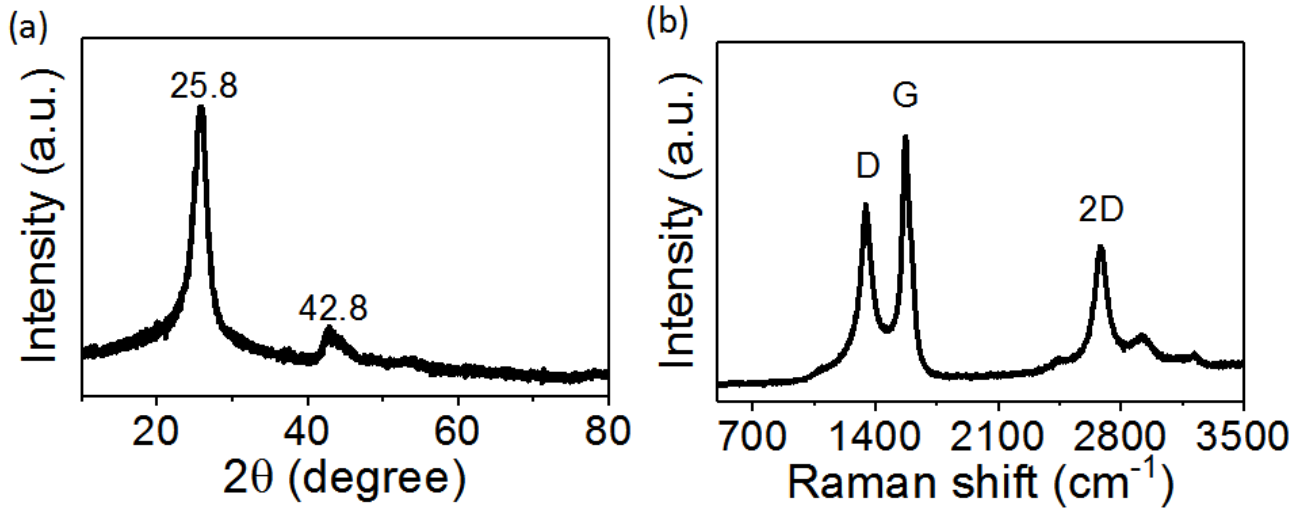


**Fig. S5.** (a) XRD pattern and (b) Raman spectrum of N,S-doped CNTs.

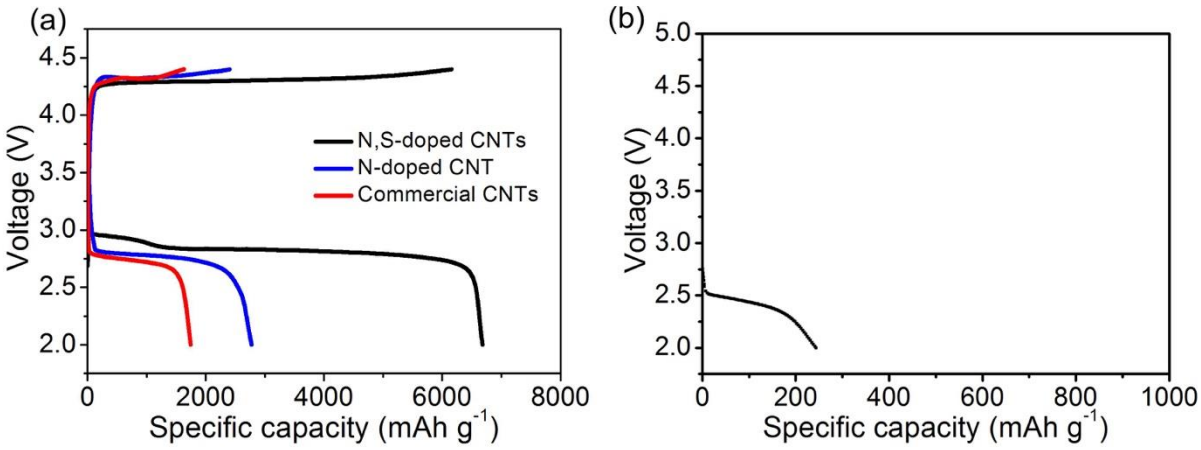


**Fig. S6.** (a) Fully discharge/charge curves of N,S-doped CNTs, N-doped CNTs, and CNTs based liquid electrolyte Li-$CO_2$ batteries, respectively. (b) Discharge curve of N,S-doped CNTs based liquid electrolyte Li-$CO_2$ battery under Ar atmosphere.

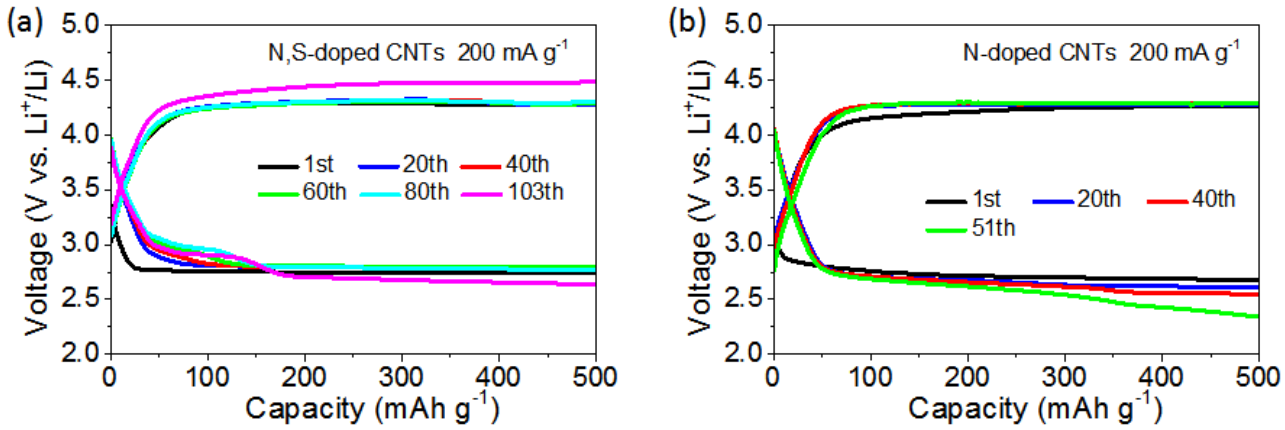


**Fig. S7.** Cyclic stability of (a) N,S-doped CNTs and N-doped CNTs based liquid electrolyte Li-$CO_2$ batteries tested at 200 mA $g^{-1}$.

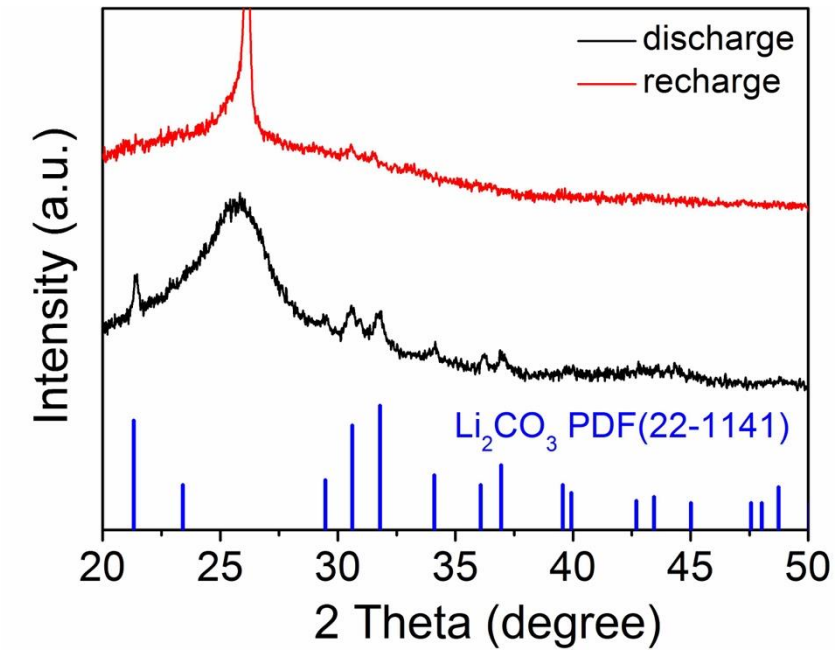


**Fig. S8.** XRD patterns of N,S-doped CNTs electrode for the liquid electrolyte Li-$CO_2$ battery tested at fully discharged and recharged states.

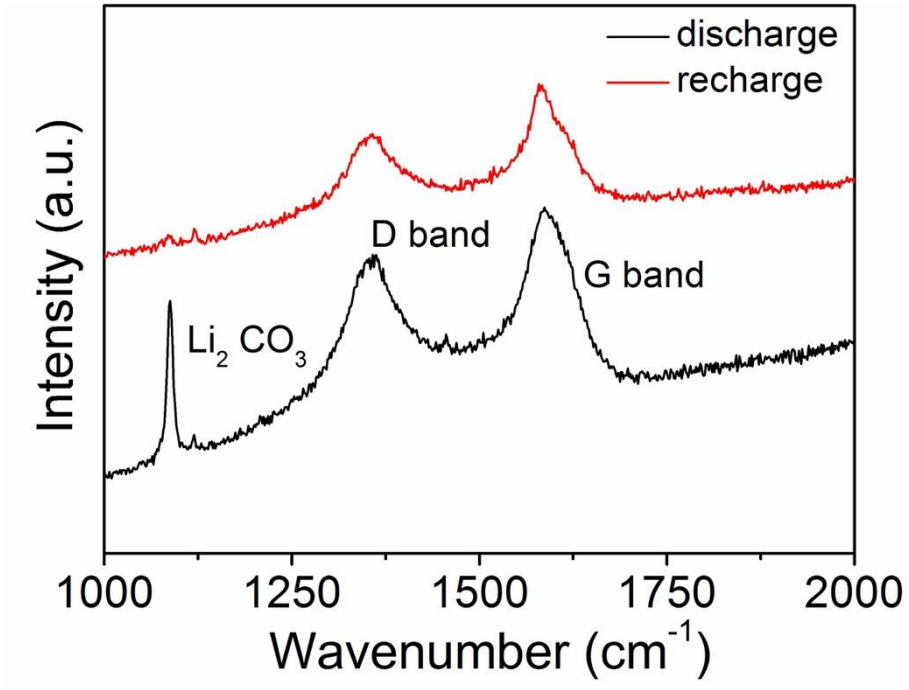


**Fig. S9.** Raman spectra of the N,S-doped CNTs based liquid electrolyte Li-$CO_2$ battery at fully discharged and recharged states.

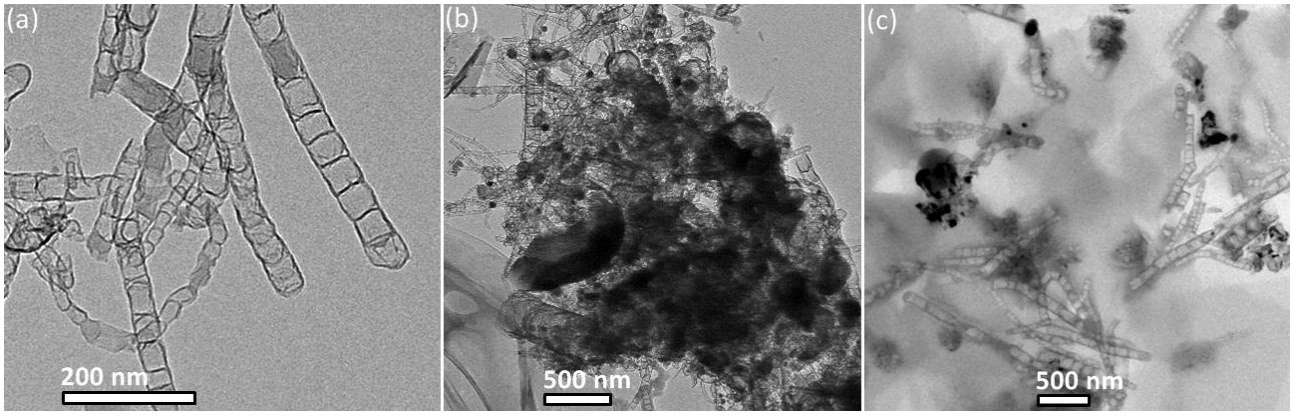


**Fig. S10.** TEM image of N,S-doped CNTs. (a) before the discharge state, (b) after fully discharged state and (c) after fully recharged state in the N,S-doped CNTs based liquid electrolyte Li-$CO_2$ battery.

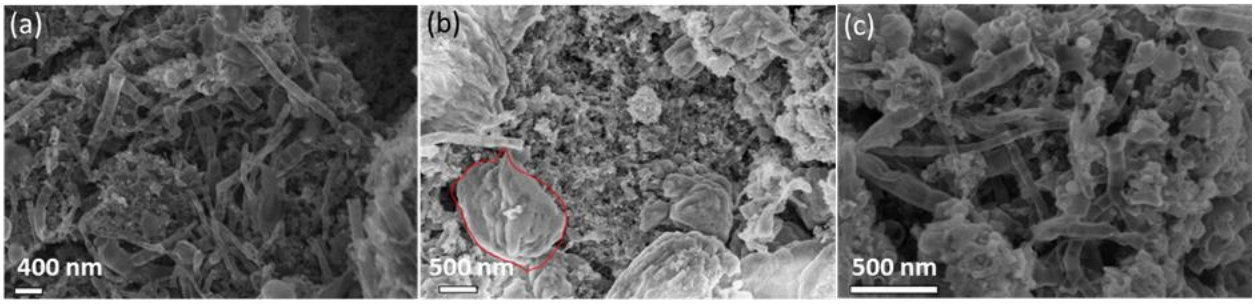


**Fig. S11.** SEM image of N,S-doped CNT cathodes. (a) Before discharged state, (b) after fully discharged state and (c) after fully recharged state in the N,S-doped CNTs based liquid electrolyte Li-$CO_2$ battery. The red circle in (b) refers to the large polymer-like discharge product.

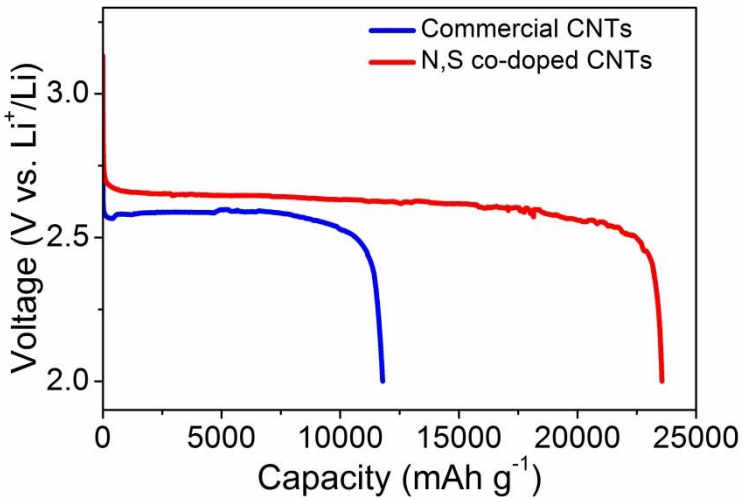


**Fig. S12.** Full discharge curves of quasi-solidus flexible Li-$CO_2$ battery with different catalysts at the current density of 200 mA $g^{-1}$.

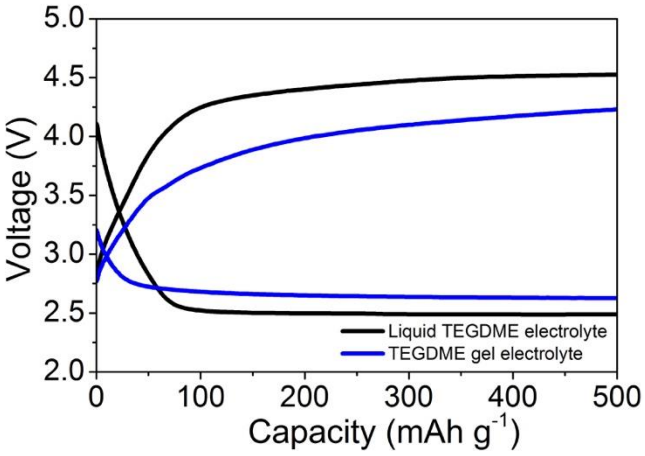


**Fig. S13.** The discharge/charge profiles for the Li-$CO_2$ batteries employing liquid and gel electrolytes containing TEGDME. A solution of 1 M LiTFSi in TEGDME was used as the electrolyte in the liquid battery.

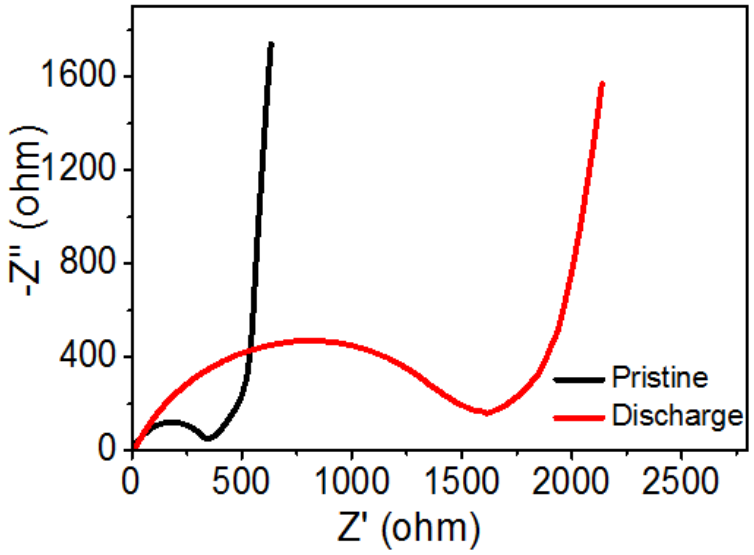


**Fig. S14.** Impedance spectra of the N,S-doped CNTs based liquid electrolyte Li-$CO_2$ cell at different states with a cut-off capacity of 2000 mAh $g^{-1}$.

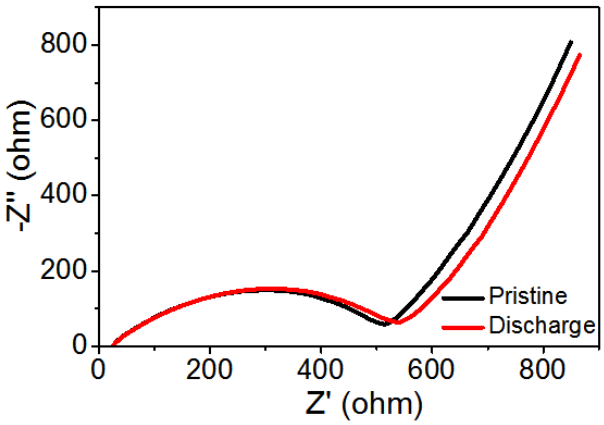


**Fig. S15.** Impedance spectra of the N,S-doped CNTs based quasi-solid-state flexible Li-$CO_2$ battery at different states with a cut-off capacity of 2000 mAh $g^{-1}$ .

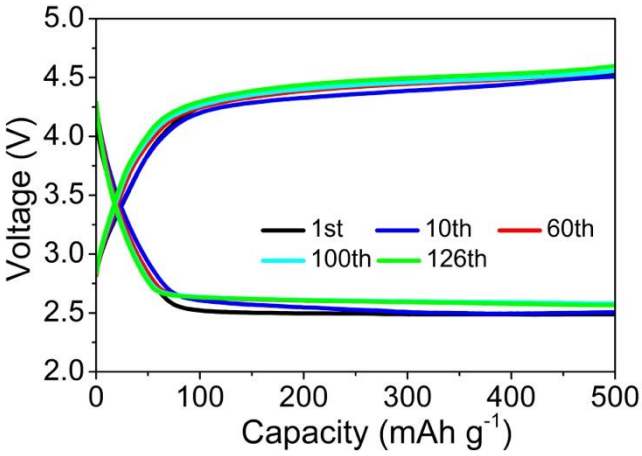


**Fig. S16.** Cyclic stability of N,S-doped CNTs based Li-$CO_2$ battery with liquid TEGDME electrolyte tested at 200 mA $g^{-1}$ with the cut-off voltages of 2.3 and 4.6 V. A solution of 1 M LiTFSi in TEGDME was used as the electrolyte.

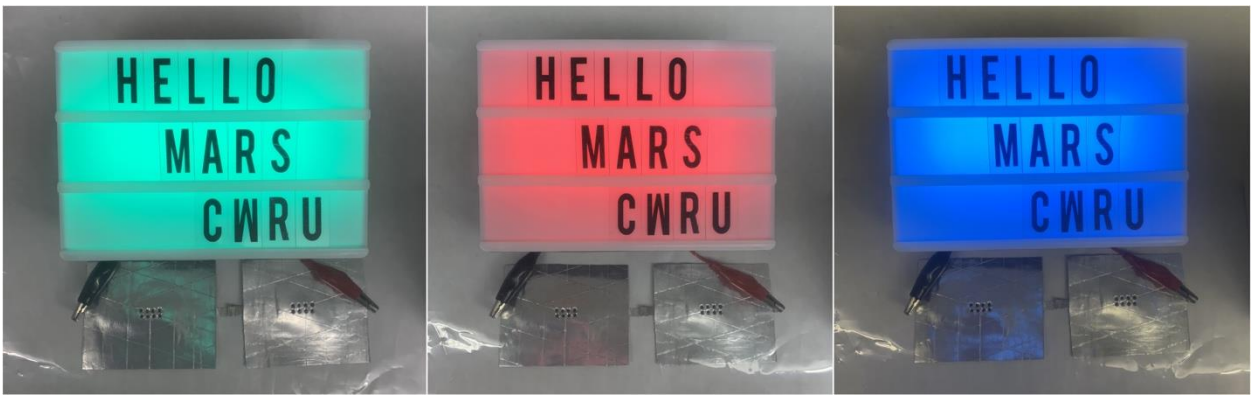


**Fig. S17.** Digital pictures of two N,S-doped CNTs based quasi-solid-state flexible Li-$CO_2$ batteries powering a cinema light box with different colors.

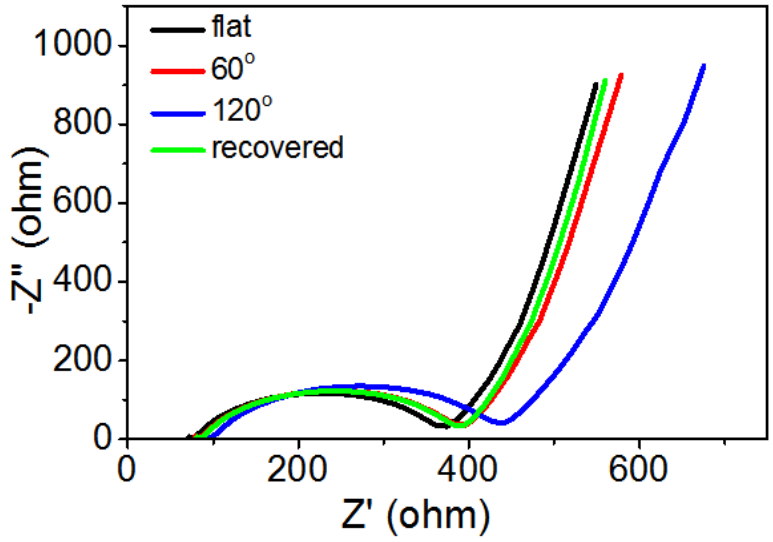


**Fig. S18.** EIS spectra of the N,S-doped CNTs based quasi-solidus Li-$CO_2$ battery under different deformation states.

**Table S1.** Comparison of N,S-doped CNTs based quasi-solidus Li-$CO_2$ battery performance with literature reports.

| **Cathode Catalyst** | **Electrolyte** | **Capacity (mAh $g^{-1}$) (at current density mA $g^{-1}$)** | **Cyclic life numbers (at current density mA $g^{-1}$ and curtailed capacity mAh $g^{-1}$)** | **Reference** |
|---|---|---|---|---|
| N,S-doped CNTs | quasi-solidus flexible gel | 23560 (200) | 538 (200, 500) | This work |
| $Mo_2C$/CNT cloth | quasi-solidus flexible gel | 3415 μAh $cm^{-2}$ (50 μA $cm^{-2}$) | 40 (80 μA $cm^{-2}$, 80 μAh $cm^{-2}$) | S1 |
| CQD/hG | Liquid | 12300 (500) | 235 (1000, 500) | S2 |
| Wrinkled N-CNTs | quasi-solidus flexible gel | 9292.3 (50) | 25 (50, 1000)<br>45 (250, 1000) | S3 |
| Ir/C Nanofiber | Liquid | 21 528 (50) | 120 (20 μA, 0.1 mAh $cm^{-2}$) | S4 |
| CNTs | Liquid-free gel | 993.3 (2.5 mA) | 100 (NA, 1000) | S5 |
| Conjugated cobalt polyphthalocyanine | Liquid | 13.6 mAh $cm^{-2}$ (0.1 mA $cm^{-2}$) | 50 (0.05 mA $cm^{-2}$, 1 mAh $cm^{-2}$) | S6 |
| graphene | Liquid | 14722 (50)<br>6600 (100) | 20 (50, 1000)<br>10 (100, 1000) | S7 |
| CNTs | Liquid | 8379 (50)<br>5786 (100) | 29 (50, 1000)<br>22 (100, 1000) | S8 |
| CNTs | quasi-solidus gel | 5139 (100) | 60 (100, 1000) | S9 |
| BN-hG | Liquid | 16033 (300) | 200 (300, 1000) | S10 |

| | | | | |
|---|---|---|---|---|
| Ni-NG | Liquid | 17625 (100) | 100 (100, 1000) | S11 |
| $MoS_2$ nanoflakes | Liquid | | 500 (500, 500) | S12 |
| MFCN | Liquid | 8827 (100) | 90 (100, 1000) | S13 |
| $Mn_2$(dobdc) | Liquid | 18022 (50) | 50 (200, 1000) | S14] |
| Cu-NG | Liquid | 14864 (100) | 50 (100, 1000) | S15 |
| Ru@Super P | Liquid | 8299 (100) | 80 (100, 1000) | S16 |
| $RuO_2$/LDO | Liquid | 5455 (100) | 60 (166, 1000) | S17 |
| Ru-Cu-GN | Liquid | 13698 (200) | 100 (200, 1000) | S18 |
| Crumpled Ir Nanosheets/CNF | Liquid | 8466.7 (200) | 400 (500,1000) | S19 |
| $RuP_2$-NPCF | Liquid | 11 951 (100) | 200 (200, 1000) | S20 |
| CNT@$RuO_2$ | Liquid | 2187 (50) | 55 (50, 500) | S21 |
| Co-doped $MnO_2$ | Liquid | 8160 (100) | 500 (100, 1000) | S22 |
| ZnS QDs/N-rGO | Liquid | 10310 (100) | 190 (400, 1000) | S23 |
| COF-Ru@CNT | Liquid | 27 348 (200) | 200 (1000, 1000) | S24 |
| $IrO_2$-N/CNT | Liquid | 4634 (100) | 316 (100, 400) | S25 |

[S1] J. Zhou, X. Li, C. Yang, Y. Li, K. Guo, J. Cheng, D. Yuan, C. Song, J. Lu, B. Wang, A quasi-solid-state flexible fiber-shaped Li-$CO_2$ battery with low overpotential and high energy efficiency. *Adv. Mater.* **31** (2019), 1804439.

[S2] Y. Jin, C. Hu, Q. Dai, Y. Xiao, Y. Lin, J. W. Connell, F. Chen, L. Dai, High-performance Li-$CO_2$ batteries based on metal-free carbon quantum dot/holey graphene composite catalysts. *Adv. Funct. Mater.* **28** (2018), 1804630.

[S3] Y. Li, J. Zhou, T. Zhang, T. Wang, X. Li, Y. Jia, J. Cheng, Q. Guan, E. Liu, H. Peng, Highly surface-wrinkled and N-doped CNTs anchored on metal wire: A novel fiber-shaped cathode toward high-performance flexible Li-$CO_2$ batteries. *Adv. Funct. Mater.* **29** (2019), 1808117.

[S4] C. Wang, Q. Zhang, X. Zhang, X. G. Wang, Z. Xie, Z. Zhou, Fabricating Ir/C nanofiber networks as Free-Standing air cathodes for rechargeable Li-$CO_2$ batteries. *Small* **14** (2018), 1800641.

[S5] X. Hu, Z. Li, J. Chen, Flexible Li-$CO_2$ batteries with liquid-free electrolyte. *Angew. Chem. Int. Ed.* **56** (2017), 5785-5789.

[S6] J. Chen, K. Zou, P. Ding, J. Deng, C. Zha, Y. Hu, X. Zhao, J. Wu, J. Fan, Y. Li, Conjugated cobalt polyphthalocyanine as the elastic and reprocessable catalyst for flexible Li-$CO_2$ batteries. *Adv. Mater.* **31** (2019), 1805484.

[S7] Z. Zhang, Q. Zhang, Y. Chen, J. Bao, X. Zhou, Z. Xie, J. Wei, Z. Zhou, The first introduction of graphene to rechargeable Li-$CO_2$ batteries. *Angew. Chem. Int. Ed.* **54** (2015), 6550-6553.

[S8] X. Zhang, Q. Zhang, Z. Zhang, Y. Chen, Z. Xie, J. Wei, Z. Zhou, Rechargeable Li-$CO_2$ batteries with carbon nanotubes as air cathodes. *Chem. Commun.* **51** (2015), 14636-14639.

[S9] C. Li, Z. Guo, B. Yang, Y. Liu, Y. Wang, Y. Xia, A rechargeable Li-$CO_2$ battery with a gel polymer electrolyte. *Angew. Chem. Int. Ed.* **56** (2017), 9126-9130.

[S10] L. Qie, Y. Lin, J. W. Connell, J. Xu, L. Dai, Highly rechargeable Lithium-$CO_2$ batteries with a boron- and nitrogen-codoped holey-graphene cathode. *Angew. Chem. Int. Ed.* **56** (2017), 6970-6974.

[S11] Z. Zhang, X. G. Wang, X. Zhang, Z. Xie, Y. N. Chen, L. Ma, Z. Peng, Z. Zhou, Verifying the rechargeability of Li-$CO_2$ batteries on working cathodes of Ni nanoparticles highly dispersed on N-doped graphene. *Adv. Sci.* **5** (2018), 1700567.

[S12] A. Ahmadiparidari, R. E. Warburton, L. Majidi, M. Asadi, A. Chamaani, J. R. Jokisaari, S. Rastegar, Z. Hemmat, B. Sayahpour, R. S. Assary, B. Narayanan, P. Abbasi, P. C. Redfern, A. Ngo, M. Vörös, J. Greeley, R. Klie, L. A. Curtiss, A. Salehi-Khojin, A long-cycle-life lithium–$CO_2$ battery with carbon neutrality. *Adv. Mater.* **31** (2019), 1902518.

[S13] Q.-C. Zhu, S.-M. Xu, Z.-P. Cai, M. M. Harris, K.-X. Wang, J.-S. Chen, Towards real Li-air batteries: A binder-free cathode with high electrochemical performance in $CO_2$ and $O_2$. *Energy Storage Mater.* **7** (2017), 209-215.

[S14] S. Li, Y. Dong, J. Zhou, Y. Liu, J. Wang, X. Gao, Y. Han, P. Qi, B. Wang, Carbon dioxide in the cage: manganese metal–organic frameworks for high performance $CO_2$ electrodes in Li-$CO_2$ batteries. *Energy Environ. Sci.* **11** (2018), 1318-1325.

[S15] Z. Zhang, Z. Zhang, P. Liu, Y. Xie, K. Cao, Z. Zhou, Identification of cathode stability in Li–$CO_2$ batteries with Cu nanoparticles highly dispersed on N-doped graphene. *J. Mater. Chem. A* **6** (2018), 3218-3223.

[S16] S. Yang, Y. Qiao, P. He, Y. Liu, Z. Cheng, J.-j. Zhu, H. Zhou, A reversible lithium-$CO_2$ battery with Ru nanoparticles as a cathode catalyst. *Energy Environ. Sci.* **10** (2017), 972-978.

[17] S.-M. Xu, Z.-C. Ren, X. Liu, X. Liang, K.-X. Wang, J.-S. Chen, Carbonate decomposition: Low-overpotential Li-$CO_2$ battery based on interlayer-confined monodisperse catalyst. *Energy Storage Mater.* **15** (2018), 291-298.

[S18] Z. Zhang, C. Yang, S. Wu, A. Wang, L. Zhao, D. Zhai, B. Ren, K. Cao, Z. Zhou, Exploiting synergistic effect by integrating ruthenium-copper nanoparticles highly co-dispersed on graphene as efficient air cathodes for Li-$CO_2$ batteries. *Adv. Energy Mater.* **9** (2019), 1802805.

[S19] Y. Xing, Y. Yang, D. Li, M. Luo, N. Chen, Y. Ye, J. Qian, L. Li, D. Yang, F. Wu, Crumpled Ir nanosheets fully covered on porous carbon nanofibers for long-life rechargeable lithium-$CO_2$ Batteries. *Adv. Mater.* **30** (2018), 1803124.

[20] Z. Guo, J. Li, H. Qi, X. Sun, H. Li, A. G. Tamirat, J. Liu, Y. Wang, L. Wang, A highly reversible long-life Li-$CO_2$ battery with a $RuP_2$-based catalytic cathode. *Small* **15** (2019), 1803246.

[21] S. Bie, M. Du, W. He, H. Zhang, Z. Yu, J. Liu, M. Liu, W. Yan, L. Zhou, Z. Zou, Carbon nanotube@$RuO_2$ as a high performance catalyst for Li–$CO_2$ batteries. *ACS Appl. Mater. Interfaces* **11** (2019), 5146−5151.

[22] B. Ge, Y. Sun, J. Guo, X. Yan, C. Fernandez, Q. Peng, A co-doped $MnO_2$ catalyst for Li-$CO_2$ batteries with low overpotential and ultrahigh cyclability. *Small* **15** (2019), 1902220.

[23] H. Wang, K. Xie, Y. You, Q. Hou, K. Zhang, N. Li, W. Yu, K. P. Loh, C. Shen, B. Wei, Realizing interfacial electronic interaction within ZnS quantum dots/N-rGO heterostructures for efficient Li–CO2 batteries. *Adv. Energy Mater*. **9** (2019), 1901806

[24] X. Li, H. Wang, Z. Chen, H. Xu, W. Yu, C. Liu, X. Wang, K. Zhang, K. Xie, K. P. Loh, Covalent-organic-framework-based Li–$CO_2$ batteries. *Adv. Mater.* **31** (2019), 1905879

[25] G. Wu, X. Li, Z. Zhang, P. Dong, M. Xu, H. Peng, X. Zeng, Y. Zhang, S. Liao, Design of an ultralong-life Li-$CO_2$ batteries with $IrO_2$ nanoparticles highly dispersed on nitrogen-doped carbon nanotubes. *J. Mater. Chem. A*, DOI: 10.1039/C9TA11028C.